Supporting Information

Morita et al. 10.1073/pnas.1107782108

SI Text

Overall Structure of HsPKS1. The obtained overall structure of HsPKS1 recapitulated the thiolase fold observed in other type III PKSs (Fig. S7*A*). As previously reported, HsPKS1 functions as a homodimeric enzyme in aqueous solution (1). The symmetric unit contained one monomer, and in the crystal, the monomer bound another monomer with a crystallographic twofold axis, thereby forming a biologically active, symmetric dimer. The active-site cavity is buried deep within each monomer, and Met147 protrudes into another monomer to form a partial wall of the active-site cavity by a cross-subunit interaction. The catalytic triad of the Cys174, His313, and Asn346 residues, which are involved in the substrate loading and the polyketide chain elongation reaction, along with decarboxylative condensation of malonyl-CoA, sits at the intersection of a traditional 16 Å-long CoA binding tunnel and the large internal cavity, in a location and orientation very similar to those of the other plant type III PKSs. The CoA-binding tunnel was also confirmed by a newly obtained crystal structure of HsPKS1 complexed with a CoA-SH molecule (Fig. S7 *A* and *B*). The overall structure of HsPKS1 is highly homologous to those of the previously reported plant type III PKSs (rmsds 0.8–0.9 Å), in which the most closely related structural homologue is that of *M. sativa* CHS (2) (PDB ID code 1CGK, Z score = 64.9, rmsd of 0.8 Å over 380 residues aligned with a sequence identity of 66%) (Fig. S7*C*).

Active-Site Architecture of HsPKS1. A comparison of the active-site of HsPKS1 and *M. sativa* CHS revealed that the backbone torsion angle of Phe275 (−119, 153) of HsPKS1, relative to that of Phe265 (−123, 131) of *M. sativa* CHS, is slightly shifted by a ϕ angle of +8° and a ψ angle of +22° with a minor displacement of its Cα-atom toward the protein surface, and the aromatic moiety of Phe275 rotates toward Thr207 by nearly 101° (Fig. S7 *D* and *E*). The conformational difference of Phe275 causes the alteration of the shape and the size of the active-site entrance and slightly expands the active-site wall near the entrance, which may account for the different substrate and product specificities of HsPKS1 (Fig. 3 *A* and *B*). Although positional differences of the so-called gatekeeper phenylalanine are often observed in the type III PKSs, this conformational change appears to be caused by the formation of a hydrogen bond between the backbone carbonyl oxygen of Phe275 and the side-chain $N\epsilon$ nitrogen of His215, on the outside of the active-site (Fig. S7*D*). This is in sharp contrast to that of *M. sativa* CHS, in which the corresponding His205 rotates toward the protein surface and is presumably prevented from forming a hydrogen bond by Tyr86 of *M. sativa* CHS, corresponding to Phe96 of HsPKS1 (Fig. S7*E*). The total area of the active-site entrance of HsPKS1 is thus 26 Å^2, which is 1.5 times larger than that of *M. sativa* CHS (17 Å^2) (Fig. 3 *A* and *B*). A widening of the active-site entrance has also been reported for the structures of the *M. sativa* F215S CHS mutant and *Rheum palmatum* benzalacetone synthase (BAS), which accept *N*-methylanthraniloyl-CoA as a starter substrate to produce *N*-methylanthraniloyltriacetic acid lactone and *N*-methyl-4-hydroxy-2(*1H*)-quinolone, respectively (3, 4). Although the residues occupy different positions at the cavity entrance from that of Phe275 in HsPKS1, the crystal structure analyses suggested that the F215S substitution of *M. sativa* CHS and the spontaneous F208L substitution of *R. palmatum* BAS expand the space at the cavity entrance to accommodate the methylamine moiety of *N*-methylanthraniloyl-CoA, and facilitate the positioning of the thioester-carbonyl moiety next to the Cys-His-Asn catalytic triad, respectively (3, 5). No other significant conformational differences, including the conservation of the so-called "coumaroyl-binding pocket," which is thought to lock the aromatic moiety of the intermediate of CHS (2), were observed in the active-site cavity of HsPKS1. We propose that HsPKS1 could principally accept the bulky substrates, such as *N*-methylanthraniloyl-CoA to produce the acridone alkaloid by the partial alteration of the size and shape of the cavity entrance rather than those of the total cavity.

Steady-State Kinetic Parameters for Enzyme Reactions. ***Wild-type HsPKS1.*** A steady-state kinetics analysis revealed $K_M = 28.8$ μM, $k_{cat} = 2.6 \times 10^{-2}$ min^{-1}, and $k_{cat}/K_M = 9.0 \times 10^2$ min^{-1} M^{-1}, for 4-coumaroyl-CoA with respect to the chalcone-forming activity (0.7% yield); $K_M = 58.4$ μM, $k_{cat} = 7.4 \times 10^{-4}$ min^{-1}, and $k_{cat}/K_M = 1.3 \times 10$ min^{-1} M^{-1}, for *N*-methylanthraniloyl-CoA with respect to the acridone-forming activity (0.03% yield); $K_M = 7.6$ μM, $k_{cat} = 4.5 \times 10^{-2}$ min^{-1}, and $k_{cat}/K_M = 5.9 \times 10^3$ min^{-1} M^{-1}, for 2-carbamoylbenzoyl-CoA with respect to the pyridoisoindole-forming activity (6.4% yield); $K_M = 17.1$ μM, $k_{cat} = 1.2 \times 10^{-2}$ min^{-1}, and $k_{cat}/K_M = 7.0 \times 10^2$ min^{-1} M^{-1}, for 3-carbamoylpicolinoyl-CoA with respect to the pyridoindolizine-forming activity (0.5% yield); $K_M = 6.8$ μM, $k_{cat} = 3.2 \times 10^{-1}$ min^{-1}, and $k_{cat}/K_M = 4.7 \times 10^4$ min^{-1} M^{-1}, for 3-carbamoyl-2-naphthoyl-CoA with respect to the pyridoisoindole-forming activity (13% yield).

HsPKS1 S348G mutant. A steady-state kinetics analysis revealed $K_M = 27.0$ μM, $k_{cat} = 3.6 \times 10^{-2}$ min^{-1}, and $k_{cat}/K_M = 1.3 \times 10^3$ min^{-1} M^{-1}, for 2-carbamoylbenzoyl-CoA with respect to the dibenzoazepine-forming activity (1.6% yield); $K_M = 40.0$ μM, $k_{cat} = 9.0 \times 10^{-2}$ min^{-1}, and $k_{cat}/K_M = 2.3 \times 10^3$ min^{-1} M^{-1}, for 2-carbamoylbenzoyl-CoA with respect to the pyridoisoindole-forming activity (3.7% yield).

SI Materials and Methods. ***Materials.*** 2-Carbamoylbenzoic and 3-carbamoylpicolic acids, and naphtho[2,3-*c*]furan-1,3-dione were obtained from Tokyo Chemical Industry Co., Ltd. Malonyl-CoA and methylmalonyl-CoA were purchased from Sigma-Aldrich. [2-^{14}C]Malonyl-CoA (53.0 mCi/mmol) was purchased from GE Healthcare. Oligonucleotides were obtained from Invitrogen. Standard chemicals were obtained from Sigma-Aldrich and Hampton Research.

Compound analysis. Online LC-ESIMS spectra were measured with an Agilent Technologies HPLC 1100 series coupled to a Bruker Daltonics esquire4000 ion trap mass spectrometer fitted with an ESI source. HRESIMS spectra were measured with an Agilent 1100 series HPLC-microTOF mass spectrometer (Bruker Daltonics), using electrospray ionization. NMR spectra were measured with JEOL JNM-A400 (400 MHz for ^{1}H and 100 MHz for ^{13}C) and JEOL ECA-500 (500 MHz for ^{1}H and 125 MHz for ^{13}C) NMR spectrometers with TMS as an external standard. HRFABMS were recorded on a JMS-700 mass spectrometer.

Synthesis of 2-carbamoylbenzoyl-CoA (6), 3-carbamoylpicolinoyl-CoA (10), and 3-carbamoyl-2-naphthoyl-CoA (12). The CoA esters were synthesized according to the published method via the synthesis of the *N*-hydroxysuccinimide (NHS) esters from the equivalent carboxylates (6).

2-Carbamoylbenzoyl-CoA (6). ^{1}H-NMR (400 MHz, D_2O): δ8.33 (1H, s), 8.11 (1H, dd, J = 2.0, 7.4 Hz), 7.99 (1H, s), 7.87 (1H, dd, J = 2.0, 7.4 Hz), 7.79 (1H, dt, J = 2.0, 7.4 Hz), 7.74 (1H, dt, J = 2.0, 7.4 Hz), 6.10 (1H, d, J = 6.4 Hz), 4.47 (1H, s), 4.25 (1H, d, J = 5.2 Hz), 4.23 (1H, d, J = 5.2 Hz), 3.99 (1H, dd, J = 4.2, 10 Hz), 3.53 (1H, dd, J = 4.2, 10 Hz), 3.47 (2H, t, J = 6.4 Hz), 3.45 (2H, t, J = 6.3 Hz), 3.25 (2H, t, J = 6.4 Hz), 2.49 (2H, t, J = 6.3 Hz), 1.06 (3H, s), 0.81 (3H, s). HRMS (FAB): found for $[C_{29}H_{41}O_{18}N_8P_3S]^+$ 914.1444; calcd. 914.1467.

3-Carbamoylpicolinoyl-CoA (10). ^{1}H-NMR (400 MHz, D_2O): δ8.60 (1H, d, 4.4 Hz), 8.27 (1H, s), 8.05 (1H, d, J = 7.8 Hz), 7.90 (1H, s), 7.52 (1H, dd, J = 4.4, 7.8 Hz), 5.84 (1H, d, J = 5.2 Hz), 4.21 (1H, s, H-7′), 3.97 (2H, s), 3.73 (1H, dd, J = 4.4, 9.0 Hz), 3.29 (1H, dd, J = 4.4, 9.0 Hz), 3.20 (2H, t, J = 6.2 Hz), 3.16 (2H, t, J = 6.0 Hz), 2.90 (2H, t, J = 6.0, 6.0 Hz), 2.16 (2H, t, J = 6.2 Hz), 1.04 (3H, s), 0.80 (3H, s). HRMS (FAB): found for $[C_{28}H_{41}O_{18}N_9P_3S]^+$ 916.1498; calcd. 916.1503.

3-Carbamoyl-2-naphthoyl-CoA (12). ^{1}H-NMR (400 MHz, D_2O): δ 8.47 (1H, s), 8.19 (1H, s), 8.18 (1H, s), 8.11 (1H, s), 7.75 (1H, dd, J = 2.0, 7.6 Hz), 7.74 (1H, dd, J = 2.0, 7.6 Hz), 7.58 (2H, dt, J = 2.0, 7.6 Hz), 6.04 (1H, d, J = 6.5 Hz), 4.44 (1H, s), 4.09 (2H, s), 3.70 (1H, dd, J = 4.0, 7.3 Hz), 3.42 (2H, t, J = 6.8 Hz), 3.36 (1H, dd, J = 4.0, 7.3 Hz), 3.09 (2H, t, J = 6.4 Hz), 2.45 (2H, t, J = 6.4 Hz), 2.31 (2H, t, J = 6.8 Hz), 0.80 (3H, s), 0.67 (3H, s). HRMS (FAB): found for $[C_{33}H_{43}O_{18}N_8P_3S]^+$ 947.1319; calcd. 947.1316.

Determination of the Novel Alkaloids Obtained by the Enzyme Reaction. ***2-Hydroxypyrido[2,1-a]isoindole-4,6-dione (7).*** LC-ESIMS (positive): Rt = 18.7 min. MS, m/z 214 $[M + H]^+$, MS/MS (precursor ion at m/z 214), m/z 171.9 $[M + H - C_2H_2O]^+$, m/z 146.0 $[M + H - C_2H_2O - CH_2]^+$. UV: λ_{max} 317 nm. ^{1}H-NMR (400 MHz, CD_3OD): δ7.90 (2H, d, J = 7.6 Hz), 7.81 (1H, t, J = 7.6 Hz), 7.67 (1H, t, J = 7.6 Hz), 6.76 (1H, s), 5.53 (1H, s). ^{13}C-NMR (100 MHz, CD_3OD): δ 173.0, 166.8, 159.4, 135.9, 135.8, 134.6, 132.2, 130.1, 118.3, 111.2, 104.9, 91.8. HRMS (FAB): found for $[C_{12}H_8O_3N]^+$ 214.0513; calcd. 214.0504.

2-Hydroxy-1,3-dimethylpyrido[2,1-a]isoindole-4,6-dione (9). LC-ESIMS (positive): Rt = 19.5 min. MS, m/z 242 $[M + H]^+$. UV: λ_{max} 231, 306 nm. ^{1}H-NMR (400 MHz, CD_3OD): δ 7.89 (1H, brd, J = 8.0 Hz), 7.82 (1H, brd, J = 8.0 Hz), 7.67 (2H, brs), 2.01 (1H, s), 1.93 (1H, s). ^{13}C-NMR (100 MHz, CD_3OD): δ 167.8, 167.5, 152.7, 137.3, 134.4, 134.4, 131.9, 131.9, 113.8, 113.4, 101.2, 11.6, 9.2. HRMS (FAB): found for $[C_{14}H_{12}O_3N]^+$ 242.0815; calcd. 242.0812.

9-Hydroxypyrido[2,3-a]indolizine-5,7-dione (11). LC-ESIMS (positive): Rt = 14.7 min. MS, m/z 215 $[M + H]^+$, MS/MS (precursor ion at m/z 215), m/z 172.8 $[M + H - C_2H_2O]^+$, m/z 147.1 $[M + H - C_2H_2O - CH_2]^+$. UV: λ_{max} 235, 324 nm. ^{1}H-NMR (400 MHz, CD_3OD): δ8.76 (1H, d, J = 4.4 Hz), 8.20 (1H, d, J = 8.0 Hz), 7.53 (1H, dd, J = 4.4,8.0 Hz), 6.97 (1H, s), 5.44 (1H, s). ^{13}C-NMR (100 MHz, CD_3OD): δ 173.5, 166.1, 158.6, 153.8, 151.4, 144.2, 135.1, 125.8, 116.8, 105.6, 93.0. HRMS (FAB): found for $[C_{11}H_7O_3N_2]^+$ 215.0457; calcd. 215.0457.

2-Hydroxybenzo[f]pyrido[2,1-a]isoindole-4,6-dione (13). LC-ESIMS (positive): Rt = 29.7 min. MS, m/z 264 $[M + H]^+$, MS/MS (precursor ion at m/z 264), m/z 222.0 $[M + H - C_2H_2O]^+$, m/z 196.0 $[M + H - C_2H_2O - CH_2]^+$. UV: λ_{max} 239, 322 nm. ^{1}H-NMR (500 MHz, DMSO): δ 8.76 (1H, s), 8.50 (1H, s), 8.18 (1H, d, J = 7.2 Hz), 8.13 (1H, d, J = 7.6 Hz), 7.80 (2H, m), 6.79 (1H, d, J = 1.6 Hz), 5.50 (1H, d, J = 1.6 Hz). ^{13}C-NMR (125 MHz, DMSO): δ 174.9, 164.6, 156.9, 137.6, 134.3, 132.3, 130.6, 130.3, 129.4, 129.4, 129.3, 128.8, 118.5, 107.1, 106.7, 88.8. HRMS (ESI): found for $[C_{16}H_{10}O_3N]^+$ 264.0664; calcd. 264.0655.

1,3-Dihydroxy-5H-dibenzo[b,e]azepine-6,11-dione (14). LC-ESIMS (positive): Rt = 25.6 min. MS, m/z 256 $[M + H]^+$, MS/MS (precursor ion at m/z 256), m/z 238.0 $[M + H - H_2O]^+$, m/z 214.0 $[M + H - C_2H_2O]^+$, m/z 172.0 $[M + H - C_4H_4O_2]^+$. UV: λ_{max} 257, 313, 363, 376 nm. ^{1}H-NMR(500 MHz, DMSO): δ 9.38 (1H, s), 8.27 (1H, s), 7.91 (1H, d, J = 7.0 Hz), 7.51 (2H, m), 7.40 (1H, d, J = 7.0 Hz), 6.85 (1H, d, J = 1.5 Hz), 5.06 (1H, d, J = 1.5 Hz). ^{13}C-NMR(125 MHz, DMSO): δ 188.5, 172.1, 165.1, 163.5, 159.8, 137.0, 136.2, 132.8, 132.7, 121.3, 121.0, 95.5, 94.6, 86.3. HRMS (ESI): found for $[C_{14}H_{10}O_4N]^+$ 256.0599; calcd. 256.0604.

Crystallization and Structure Determination of the HsPKS1 Complexed with CoA-SH. The HsPKS1 crystals, complexed with CoA-SH, were obtained by the same crystallization method as in the case of the apo crystals of HsPKS1, except for the cocrystallization with 2 mM CoA-SH (7). The crystals were transferred into the reservoir solution with 12% (v/v) glycerol and 14% (w/v) PEG400 as a cryoprotectants, and then were flash-cooled at 100 K in a nitrogen-gas stream. X-ray diffraction datasets were collected at SPring-8 beamline BL24XU (wavelength, 0.82656 Å), using a Rigaku R-AXIS V imaging-plate area detector. Crystal data and intensity statistics are summarized in Table S1. The crystal belonged to the space group $P2_12_12_1$, with unit-cell parameters a = 75.6 Å, b = 84.1 Å, c = 137.7 Å, $\alpha = \beta = \gamma = 90.0°$, and contained two molecules in the asymmetric unit. Data were indexed, integrated and scaled with HKL2000 (8). The structure was solved by the same procedure as that used for the model refinement of the HsPKS1 apo structure, except for the use of the final model of the wild-type apo structure as the search model in the molecular replacement methods. The $2F_o$-F_c and F_o-F_c maps indicated the presence of a portion of the CoA-SH molecule in a monomer A, and the CoA-SH molecule was manually fit into the visible electron density. The final model consists of residues 20–399 of monomer A, 20–399 of monomer B, one molecule of CoA-SH, two molecules of SO_4, and 227 molecules of water. Details of the data collection, processing, and structure refinement are summarized in Table S1. The qualities of the final models were assessed with PROCHECK (9). A total of 91.1% of the residues in the CoA-SH complexed HsPKS1 structure are in the most favored regions of Ramachandran plot, 8.6% in the additional allowed regions, and 0.3% in generously allowed region.

Site-directed mutagenesis. The expression plasmids of HsPKS1 single mutant (S348G, S348C, S348T, and S348V) were constructed with the QuikChange Site-Directed Mutagenesis Kit (Stratagene), according to the manufacture's protocol, using the HsPKS expression plasmid (1) as a template and a pair of primers as follows (mutated codons are underlined): S348G (5′-CGGCAACATG<u>GGA</u>AGCGC CTCAGTACTGTTTG-TTTTGG-3′ and 5′-CCAAAACAAACAGTACTGAGG-CGCT<u>TCC</u>CA TGTTGCCG-3′), S348C (5′-CGGCAACAT-G<u>TGC</u>AGCGCCTCAGTACTGTTTGTTTTGG-3′ and 5′-CCA-AAACAAACAGTACTGAGGCGCT<u>GCA</u>CATGTTGCCG-3′), S348T (5′-CGGCA ACATG<u>ACA</u>AGCGCCTCAGTACTG-TTTGTTTTGG-3′ and 5′-CCAAAACAAACAGTACT GAGG-CGCT<u>TGT</u>CATGTTGCCG-3′) and S348V (5′-CGGCAA-CATG<u>GTA</u>AGCGCCTCAGT ACTGTTTGTTTTGG-3′ and 5′-CCAAAACAAACAGTACTGAGGCGCT<u>TAC</u>CATGTTGCC G-3′). The expression plasmids of HsPKS1 double mutant (F225G/S348G, F225A/S348G, F225S/S348G, F225C/S348G, F225L/S348G, F225H/S348G, F225Y/S348G and F225W/S348G) were also constructed by the same procedure as that for the HsPKS1 single mutant, except for using the HsPKS1 S348G expression plasmid as a template and a pair of primers as follows

(mutated codons are underlined): F225G/S348G (5′-GGCTCTGCTCTCGGCGGCGATGGCGCAGC-3′ and 5′-GCTGCGCCATCGCCGCCGA GAGCAGAGCC-3′), F225A/S348G (5′-GGCTCTGCTCTCGCCGGCGATGGCGCAGC-3′ and 5′-GCTGCGCCATCGCCGGCGAGAGCAGAGCC-3′), F225S/S348G (5′-GGCTCTGCTC TCTCCGGCGATGGCGCAGC-3′ and 5′-GCTGCGCCATCGCCGGAGAGAGCAGAGCC-3′), F225C/S348G (5′-GGCTCTGCTCTCTGCGGCGATGGCGCAGC-3′ and 5′-GCTGCGCCATC GCCGCAGAGAGCAGAGCC-3′), F225L/S348G (5′-GGCTCTGCTCTCCTCGGCGATGGC GCAGC-3′ and 5′-GCTGCGCCATCGCCGAGGAGAGCAGAGCC-3′), F225H/S348G (5′-GG CTCTGCTCTCCACGGCGATGGCGCAGC-3′ and 5′-GCTGCGCCATCGCCGTGGAGAGC AGAGCC-3′), F225Y/S348G (5′-GGCTCTGCTCTCTACGGCGATGGCGCAGC-3′ and 5′-GC TGCGCCATCGCCGTAGAGAGCAGAGCC-3′) and F225W/S348G (5′-GGCTCTGCTCTCT GGGGCGATGGCGCAGC-3′ and 5′-GCTGCGCCATCGCCCCAGAGAGCAGAGCC-3′).

Bioassay procedure. For the antibacterial assay, methicillin-susceptible *Staphylococcus aureus* (MSSA), *Escherichia coli*, and *Bacillus cereus* were cultured overnight in LB medium at 37 °C. A 10 μL aliquot of the cultured cells was resuspended in 1 mL of Mueller Hinton medium, and 100 μL portions of the cell suspensions were then seeded in each 96-well plate (2×10^4 colony forming units (CFU)/well). A 2 μL portion of the test solution (samples were dissolved in DMSO) was subsequently added, at final concentrations of 100, 50, 25, 12.5, and 6.3 μg/mL for 2-hydroxypyrido[2,1-*a*]isoindole-4,6-dione (**7**), and 24, 12, 6, 3, and 1.5 μg/mL for 1,3-dihydroxy-5*H*-dibenzo[*b*,*e*]azepine-6,11-dione (**14**), respectively, and the plates were incubated for 16 hours at 37 °C. Ampicillin (final concentrations of 16, 8, 4, 2, and 1 μg/mL) and saline solution (final percentages of 9.0×10^{-3}, 4.5×10^{-3}, 2.3×10^{-3}, 1.1×10^{-3}, 0.6×10^{-3}%) were used as positive and negative control experiments, respectively. The experiments were performed in duplicate.

For the cytotoxicity assay, P388 murine leukemia cells were cultured in RPMI 1640 (Wako Chemicals) medium supplemented with 10 μg/mL of penicillin/streptomycin (Invitrogen) and 10% fetal bovine serum (MP Biomedicals), at 37 °C under a 5% CO_2 atmosphere. To each well of a 96-well microplate containing a 100 μL of 1×10^4 cells/mL tumor cell suspension, a 100 μL aliquot of test solution (samples were dissolved in DMSO) was added, and the plates were incubated for 96 h. After the addition of 50 μL of 3-(4,5-dimethyl-2-thiazolyl)-2,5-diphenyl-2*H*-tetrazolium bromide (MTT) solution (1 mg/mL) to each well, the plates were incubated for 3 h under the same conditions. The mixtures were centrifuged, and the supernatants were removed. The precipitates thus obtained were dissolved in DMSO, and the absorbance at 570 nm was measured with a microplate reader.

1. Wanibuchi K, et al. (2007) An acridone-producing novel multifunctional type III polyketide synthase from *Huperzia serrata*. *FEBS J* 274:1073–1082.
2. Ferrer JL, Jez JM, Bowman ME, Dixon RA, Noel JP (1999) Structure of chalcone synthase and the molecular basis of plant polyketide biosynthesis. *Nat Struct Biol* 6:775–784.
3. Jez JM, Bowman ME, Noel JP (2002) Expanding the biosynthetic repertoire of plant type III polyketide synthases by altering starter molecule specificity. *Proc Natl Acad Sci USA* 99:5319–5324.
4. Abe I, Abe T, Wanibuchi K, Noguchi H (2006) Enzymatic formation of quinolone alkaloids by plant type III polyketide synthase. *Org Lett* 8:6063–6065.
5. Morita H, et al. (2010) A structure-based mechanism for benzalacetone synthase from *Rheum palmatum*. *Proc Natl Acad Sci USA* 107:669–673.
6. Stöckigt J, Zenk MH (1975) Chemical syntheses and properties of hydroxycinnamoyl-coenzyme A derivatives. *Z Naturforsch* 30c:352–358.
7. Morita H, et al. (2007) Crystallization and preliminary crystallographic analysis of an acridone-producing novel multifunctional type III polyketide synthase from *Huperzia serrata*. *Acta Crystallogr Sect F Struct Biol Cryst Commun* 63:576–578.
8. Otwinowski Z, Minor W (1997) Processing of X-ray diffraction data collected in oscillation mode. *Methods Enzymol* 276:307–326.
9. Laskowski RA, MacArthur MW, Moss DS, Thornton JM (1993) PROCHECK: A program to check the stereochemical quality of protein structures. *J Appl Crystallogr* 26:283–291.

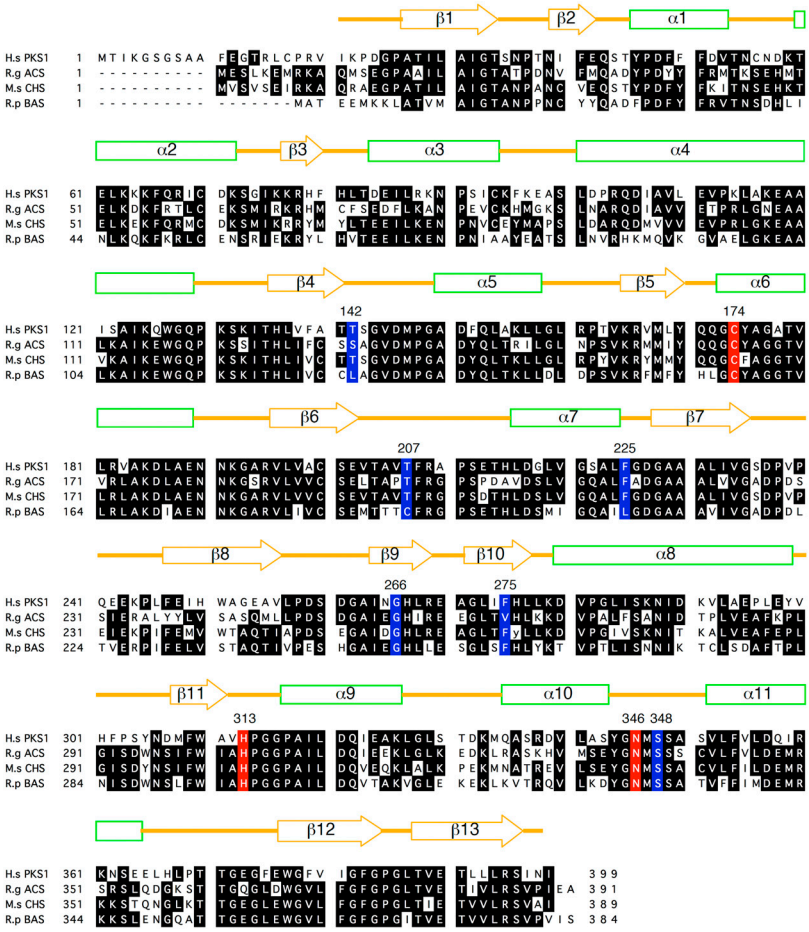

Fig. S1. Comparison of the primary sequence of HsPKS1 and other type III PKSs. The secondary structures of HsPKS1 are delineated: α-helices (green rectangles), β-strands (orange arrows), and loops (orange, bold lines) are diagrammed. The catalytic triad Cys-His-Asn residues and the residues thought to be crucial for the functional diversity of the type III PKSs are colored red and blue, respectively (numbering according to HsPKS1). Abbreviations (GeneBank accession numbers): H.s PKS1, *Huperzia serrata* HsPKS1 (AB495007); R.g ACS, *Ruta graveolens* ACS (CAC14058); M.s CHS, *Medicago sativa* CHS (Os07-g17010.1_ORYZA); R.p BAS, *Rheum palmatum* BAS (AAK82824).

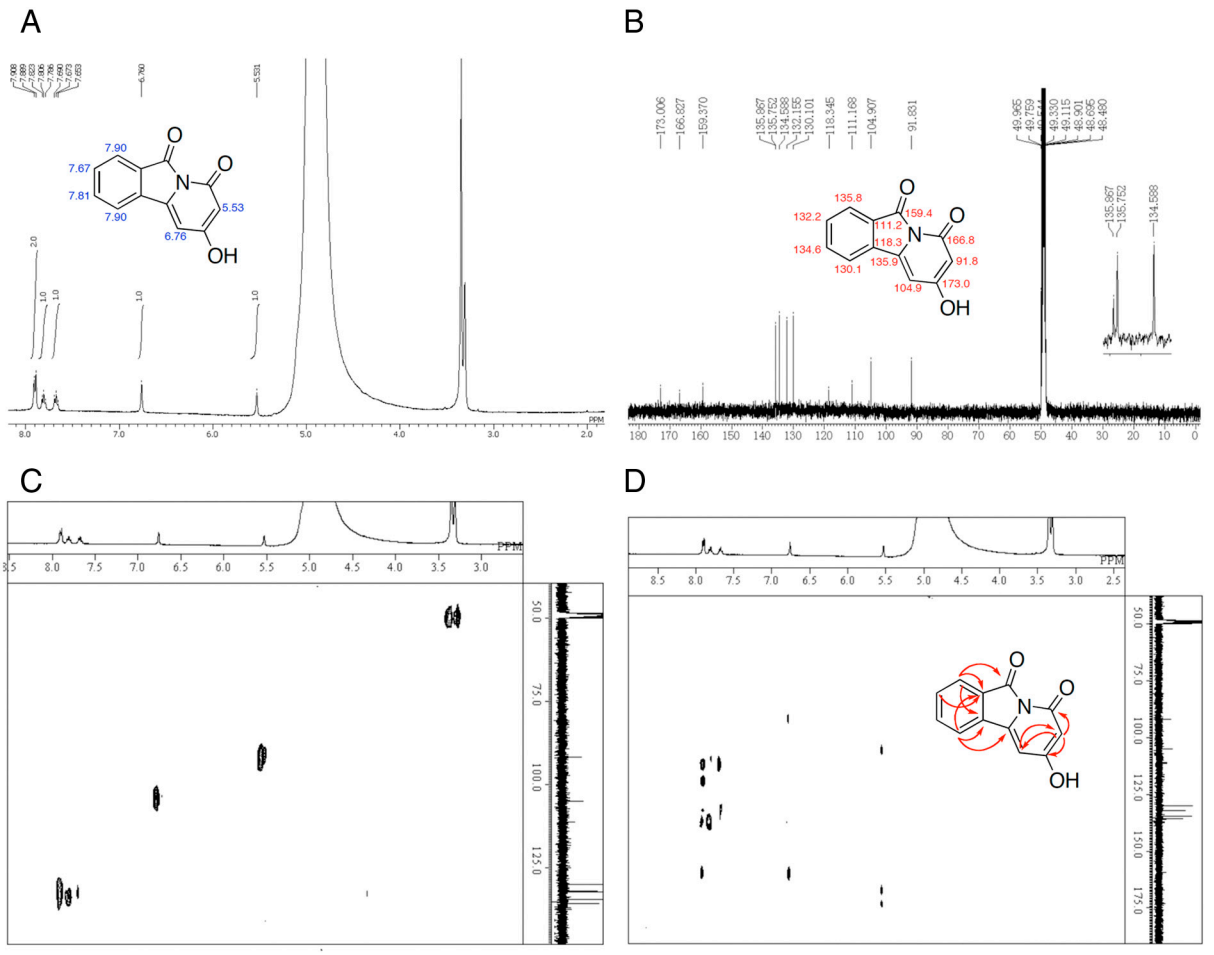

Fig. S2. NMR spectra of 2-hydroxypyrido[2,1-*a*]isoindole-4,6-dione. (*A*) ^{1}H NMR spectrum (in CD_3OD, 400 MHz). (*B*) ^{13}C NMR spectrum (in CD_3OD, 100 MHz). (*C*) HMQC spectrum (in CD_3OD, 400 MHz). (*D*) HMBC spectrum (in CD_3OD, 400 MHz).

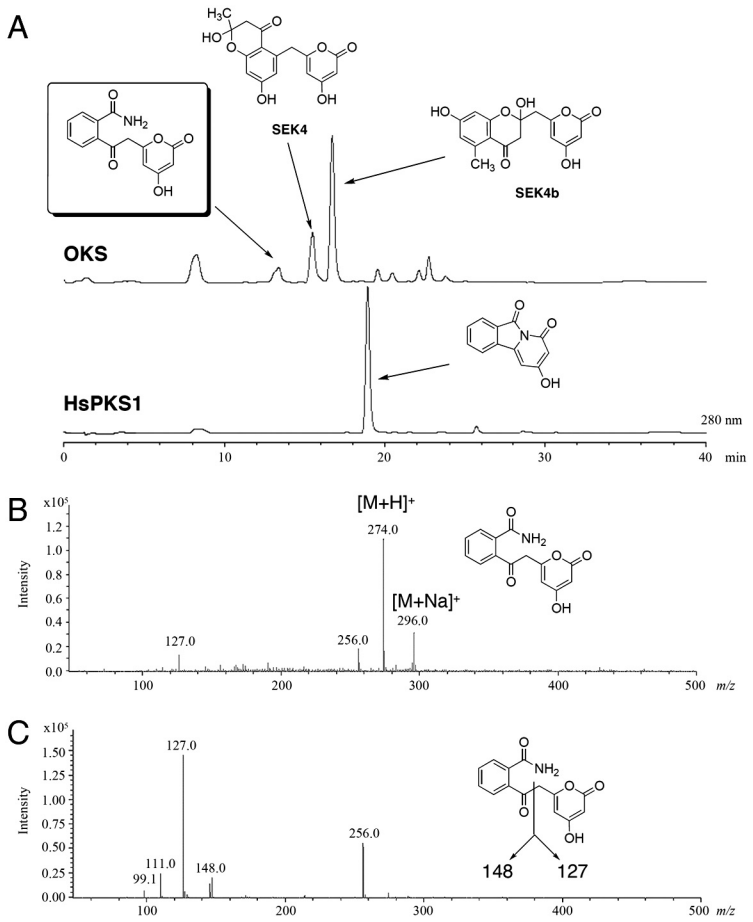

Fig. S3. Enzyme reaction products of *A. arborescens* OKS and HsPKS1 by using 2-carbamoylbenzoyl-CoA and malonyl-CoA as the substrates. (*A*) HPLC elution profiles. (*B*) MS and (*C*) MS/MS (precursor ion at m/z 274) spectra of the tetraketide pyrone produced by OKS.

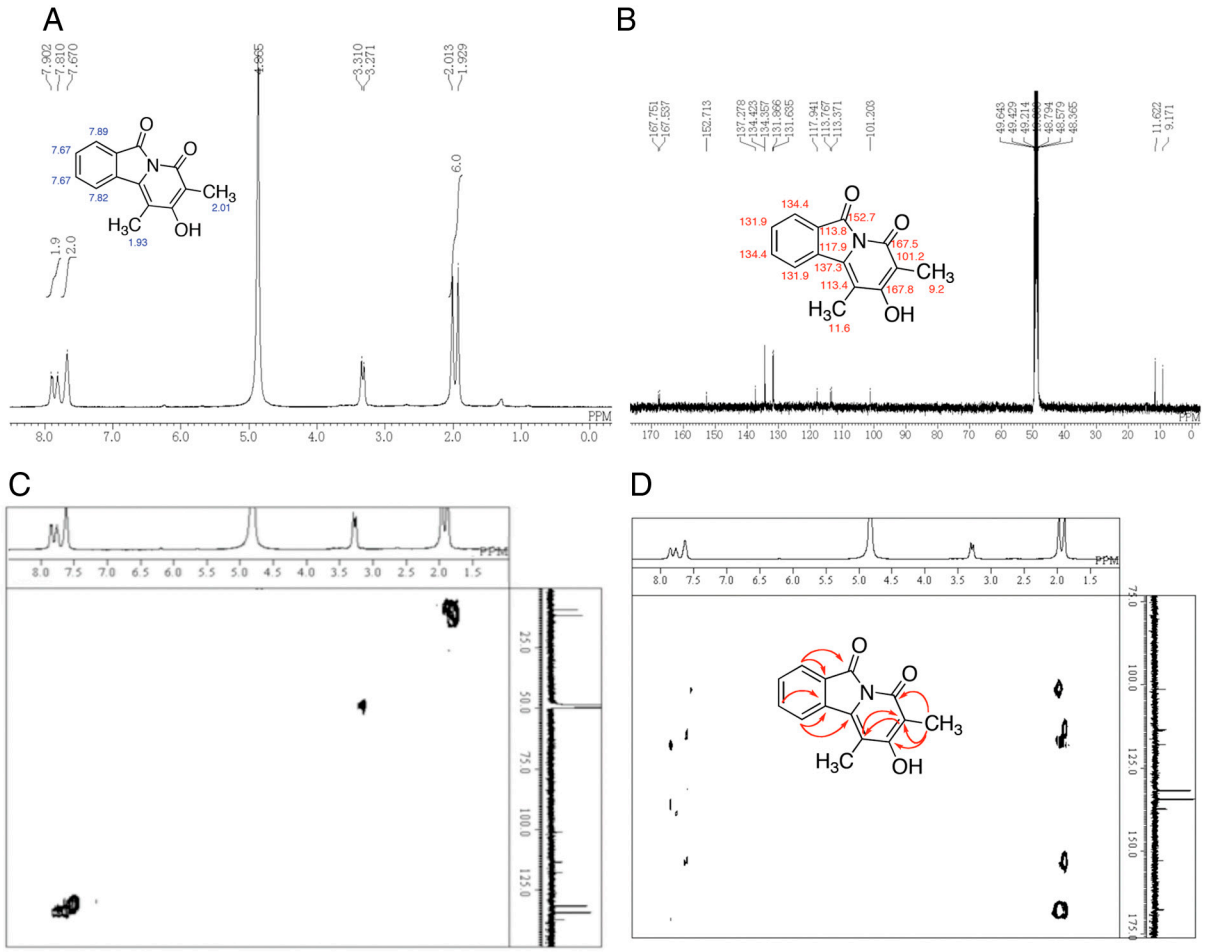

Fig. S4. NMR spectra of 2-hydroxy-1,3-dimethylpyrido[2,1-*a*] isoindole-4,6-dione. (*A*) ^{1}H NMR spectrum (in CD_3OD, 400 MHz). (*B*) ^{13}C NMR spectrum (in CD_3OD, 100 MHz). (*C*) HMQC spectrum (in CD_3OD, 400 MHz). (*D*) HMBC spectrum (in CD_3OD, 400 MHz).

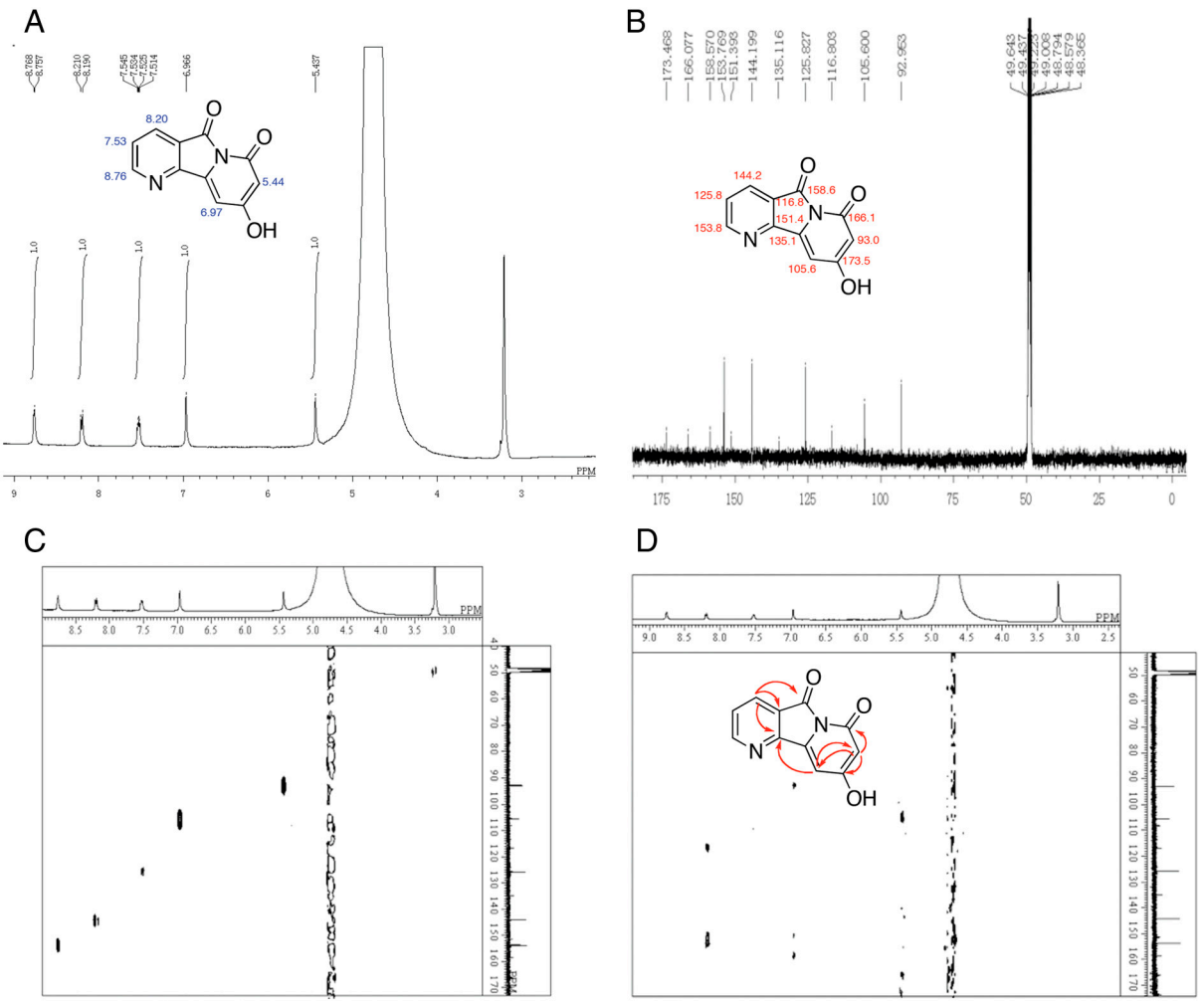

Fig. S5. NMR spectra of 9-hydroxypyrido[2,3-*a*]indolizine-5,7-dione. (*A*) ^{1}H NMR spectrum (in CD_3OD, 400 MHz). (*B*) ^{13}C NMR spectrum (in CD_3OD, 100 MHz). (*C*) HMQC spectrum (in CD_3OD, 400 MHz). (*D*) HMBC spectrum (in CD_3OD, 400 MHz).

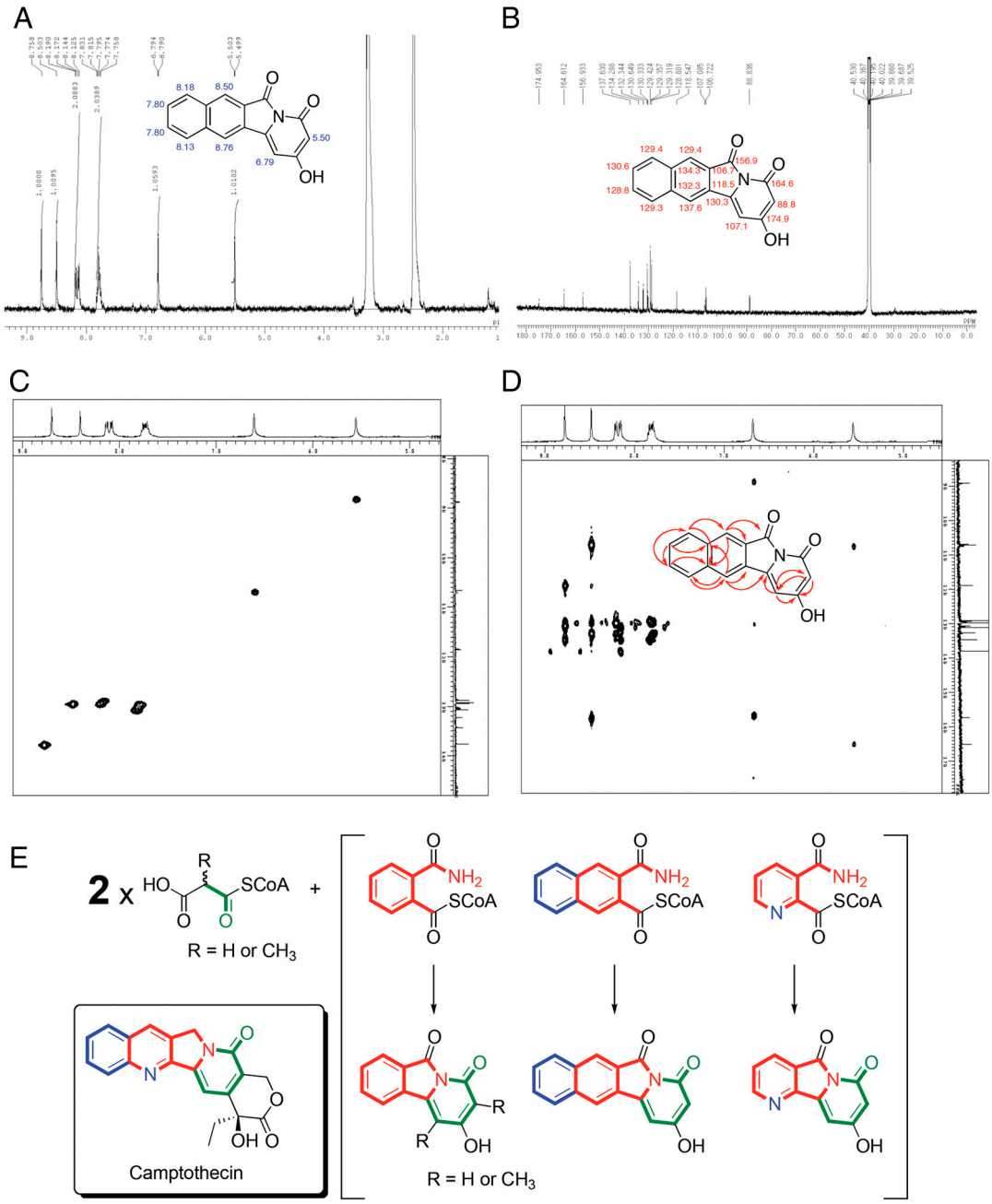

Fig. S6. NMR spectrum of 2-hydroxybenzo[*f*]pyrido[2,1-*a*]isoindole-4,6-dione. (*A*) x^1H NMR spectrum (in CD_3OD, 500 MHz). (*B*) ^{13}C NMR spectrum (in d_6-DMSO 125 MHz). (*C*) HMQC spectrum (in CD_3OH, 500 MHz). (*D*) HMBC spectrum (in CD_3OD, 500 MHz). (*E*) Comparison of the structure of camptothecin and the pyridoisoindole and pyridoindolizine alkaloids, obtained by the enzyme reaction catalyzed by HsPKS1.

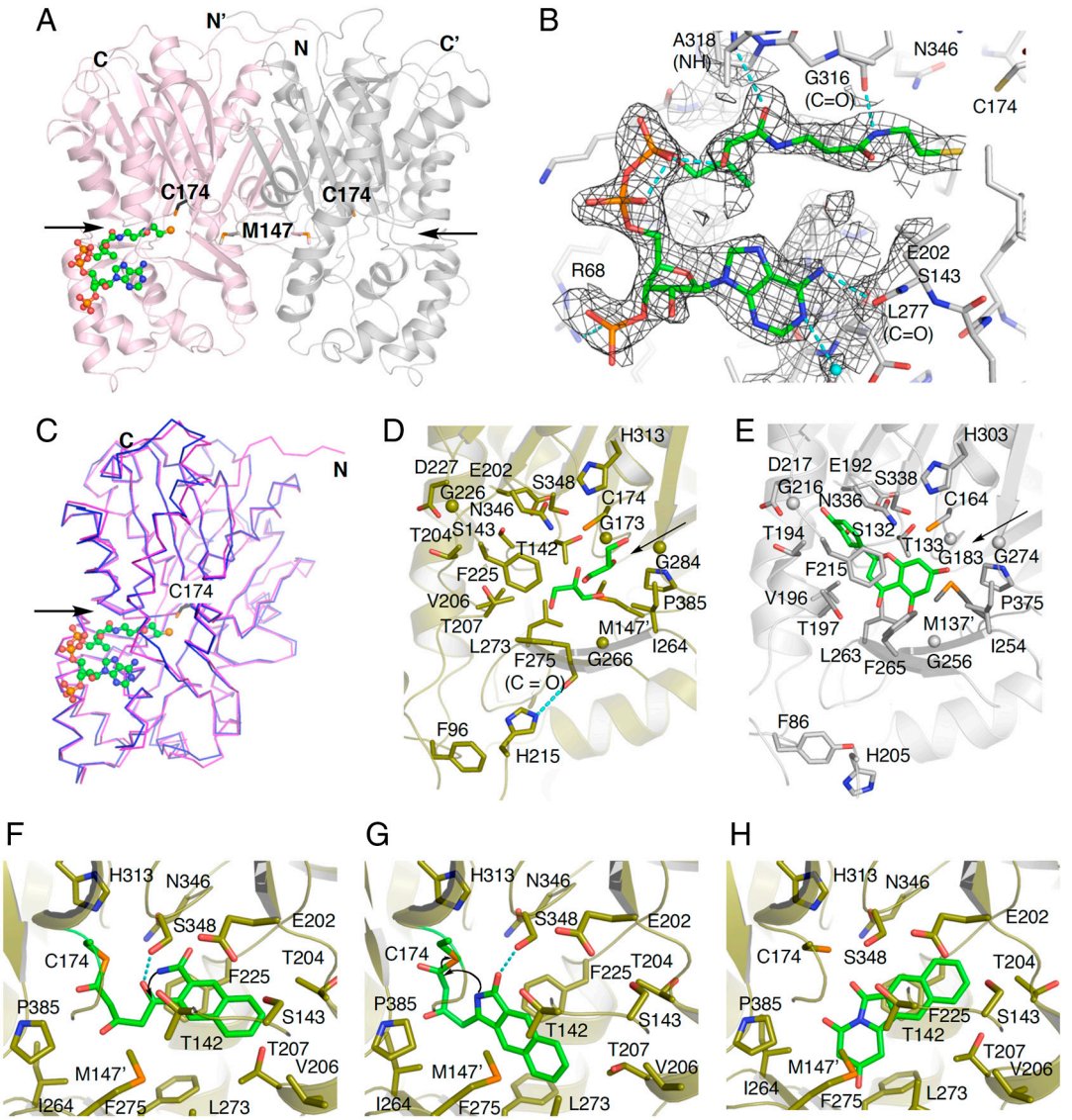

Fig. S7. Overall structure of HsPKS1. (*A*) Schematic representations of the apo structure of HsPKS1. Arrows indicate the substrate entrance in each monomer. The catalytic Cys174 and Met147 residues, which form a partial wall of the active-site cavity of another monomer, are indicated by stick model. The CoA-SH molecule bound in the HsPKS1 structure is depicted by a green ball-and-stick model. (*B*) The F_o-F_c density map of the CoA-SH molecule in the HsPKS1 structure, contered at 1.0 sigma. The water molecule and the hydrogen bonds are indicated with light-blue sphere and dotted lines, respectively. (*C*) Comparison of HsPKS1 (purple) and *M. sativa* CHS (blue). The catalytic Cys174 and the bound CoA-SH in HsPKS1 are shown as black stick and green ball-and-stick models, respectively. (*D* and *E*) Ribbon representation of the crystal structure of (*D*) wild-type HsPKS1 and (*E*) *M. sativa* CHS. The glycerol and naringenin molecules bound to the active-site cavities of wild-type HsPKS1 and *M. sativa* CHS, respectively, are shown as green stick models. The hydrogen bond is indicated with a light-blue dotted line. Arrows indicate the active-site entrance in each cavity. (*F–H*) Proposed mechanism for the formation of 2-hydroxybenzo[*f*] pyrido[2,1-*a*] isoindole-4,6-dione by wild-type HsPKS1. Three-dimensional model of (*F*) the triketide linear intermediate, (*G*) the 5-hydroxyheterpentacyclized triketide intermediate and (*H*) the partially cyclized triketide intermediate, covalently bound to the catalytic Cys174 of HsPKS1. The intermediate models are highlighted with green stick models.

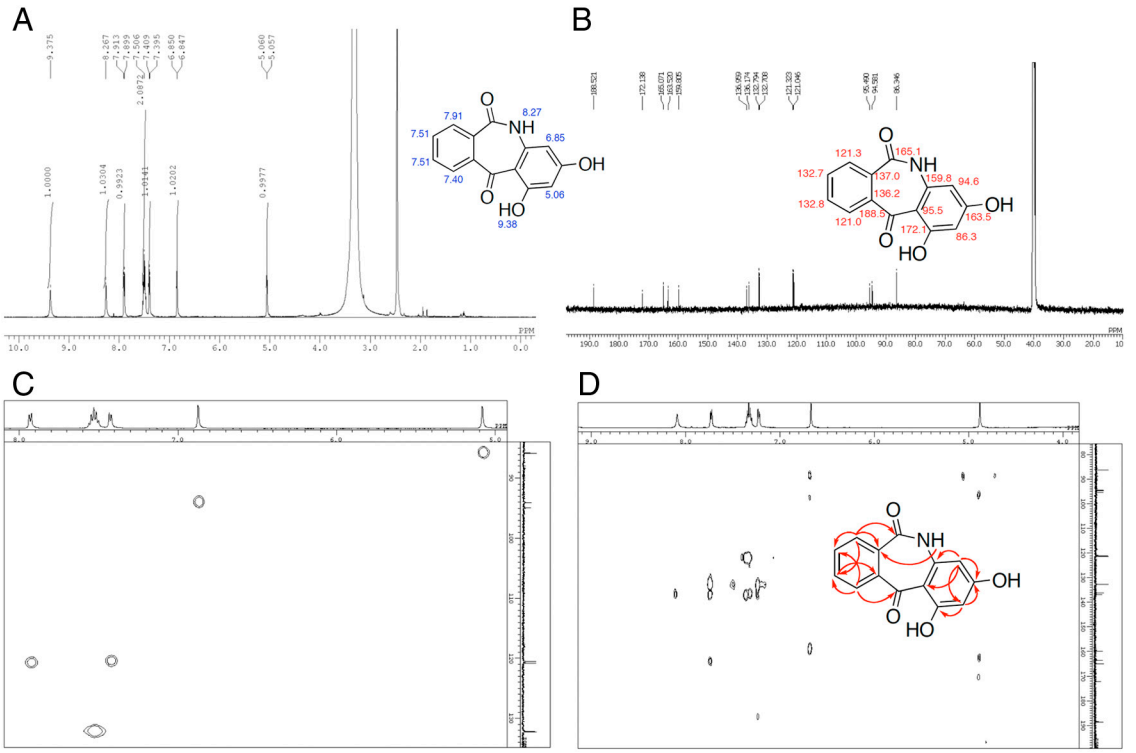

Fig. S8. NMR spectra of 1,3-dihydroxy-5*H*-dibenzo[*b*, *e*]azepine-6,11-dione. (*A*) ^{1}H NMR spectrum (in d_6-DMSO, 500 MHz). (*B*) x^{13}C NMR spectrum (in d_6-DMSO, 125 MHz). (*C*) HMQC spectrum (in d_6-DMSO, 500 MHz). (*D*) HMBC spectrum (in d_6-DMSO, 500 MHz).

Table S1. Data collection and refinement statistics

Data collection	HsPKS1	HsPKS1_CoA-SH
Space group	$I2_12_12_1$	$P2_12_12_1$
Unit-cell		
a, *b*, *c* (Å)	73.3, 85.0, 137.7	75.6, 84.1, 137.7
α, β, γ (°)	90.0, 90.0, 90.0	90.0, 90.0, 90.0
Resolution (Å)	30.0–2.0 (2.07–2.00)	30.0–2.2 (2.28–2.20)
Unique reflections	27623	42570
Redundancy	7.1 (7.1)	6.6 (5.9)
Completeness (%)	100.0 (100.0)	99.7 (98.3)
$\langle I/(\sigma I)\rangle$	49.2 (10.8)	34.3 (9.2)
R_{sym} (%) *	5.6 (28.4)	9.2 (28.8)
Refinement		
Resolution (Å)	2.0	2.2
R_{cryst}/R_{free} (%) †	21.1/23.4	22.8/26.1
No. atoms		
Protein	2933	5840
Water	169	228
Ligand	17	58
B-factors (Å^2)		
Protein	26.9	23.4
Water	28.9	24.7
Ligand	56.5	46.6
R.m.s deviations		
Bond lengths (Å)	0.011	0.012
Bond angles (°)	1.5	1.6

Values in parentheses are for the highest resolution shell.

*$R_{sym} = S_h S_i |I(h)_i - \langle I(h)\rangle| / S_h S_i I(h)_i$, where $I(h)$ is the intensity of refraction h, S_h is the sum over all reflections and S_i is the sum over i measurements of reflection h.

†R_{free} was calculated with 5% of data excluded from refinement.